Study on the Defects Detection in Composites by Using Optical Position and Infrared Thermography

Koo-Ahn Kwon*, Hee-Sang Park**†, Man-Yong Choi*, Jeong-Hak Park* and Won Jae Choi*

Abstract Non-destructive testing methods for composite materials (e.g., carbon fiber-reinforced and glass fiber-reinforced plastic) have been widely used to detect damage in the overall industry. This study detects defects using optical infrared thermography. The transient heat transport in a solid body is characterized by two dynamic quantities, namely, thermal diffusivity and thermal effusivity. The first quantity describes the speed with thermal energy diffuses through a material, whereas the second one represents a type of thermal inertia. The defect detection rate is increased by utilizing a lock-in method and performing a comparison of the defect detection rates. The comparison is conducted by dividing the irradiation method into reflection and transmission methods and the irradiation time into 50 mHz and 100 mHz. The experimental results show that detecting defects at 50 mHz is easy using the transmission method. This result implies that low-frequency thermal waves penetrate a material deeper than the high-frequency waves.

Keywords: Optical Infrared Thermography, Lock-in Method, Composite Materials, Quantitative Defects Detection

1. Background

The utilization of composite materials is currently being expanded throughout the industry. The composite materials are the ones to be artificially made to ensure that two or more materials maintain their macroscopic characteristics and complement each other for excellent physical properties. Typical examples of the composite materials are CFRP (carbon fiber reinforced plastic) and GFRP (glass fiber reinforced plastic). These composites have widely been used in a variety of areas such as aerospace, shipping, automobiles and railways [1].

In this connection, a research on the non-destructive testing to measure the defects of composite materials has actively been conducted. In this paper, we conducted a study to quantify the sizes of the defects in CFRP and GFRP composites by using optical lock-in infrared

thermography among non-destructive testing methods. The infrared thermography (IRT) has some advantages in that it can help to detect defects in a non-contact state with the use of the infrared emission energy of the object, and is very useful in detecting inclusion detects of CFRP and GFRP composites. In addition, it is considered to be a very appropriate method for detecting defects of a large structure as a testing method that can relatively easily detect defects in a movable state at the site [2].

2. Materials and Devices

2.1. Specimens

The composites-based specimens of inclusion defects used in this study are as follows. To detect defects inside the inclusion of composite materials by using infrared thermography, this

study manufactured and compared inclusion defect (teflon film) specimen according to the kinds of defects (shape), defect size and defect depth in laminate, and the composite materials used for this experiment were as follows: Firstly, as a material widely used for aerospace, Cycom 5276-1 G40-800-24K UD tape, created by synthesizing Cycom 5276-1 epoxy resin with high-strength T800 oneway carbon fiber, was used. Secondly, as a material applied to electronic PCB substrates and wind power-generation blades, SKY FLEX UGN 150, created by synthesizing epoxy resins with one-way E-glass fiber, was also used for comparative.

Fig. 1 shows CFRP specimen of inclusion defects, which was laminated with eight layers, and star and oval-shaped defects were inserted into CFRP composites 300 mm in length and breadth with a thickness of 1.4 mm (8 layers) by teflon films inserted in the left side at a depth of 25% and in the right side at a depth of 50% based on the center line.

GFRP specimen of inclusion defects of Fig. 2 was laminated with 16 layers and produced to have the same thickness as CFRP specimen, and star, circular and oval-shaped defects were inserted in the left side at a depth of 12.5% and in the right side at a depth of 62.5%, respectively with Teflon films. As shown in Fig. 3, a matt black paint was applied so that CFRP and GFRP specimens of inclusion defects can meet the condition close to an emissivity rating of 0.95 [3,4].

2.2. Experimental Device Configuration

The method for detecting defects in composite materials using infrared thermography is largely divided into passive method and active method, and an experimental device was configured using an active optical infrared thermography technique.
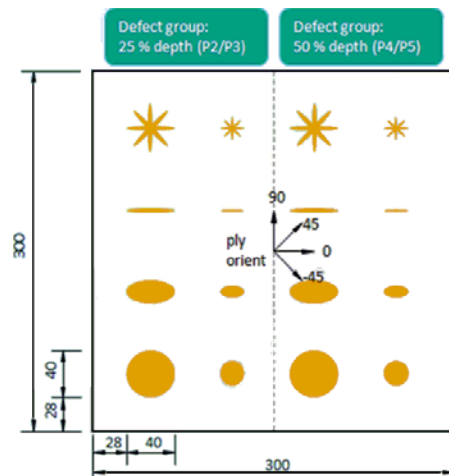

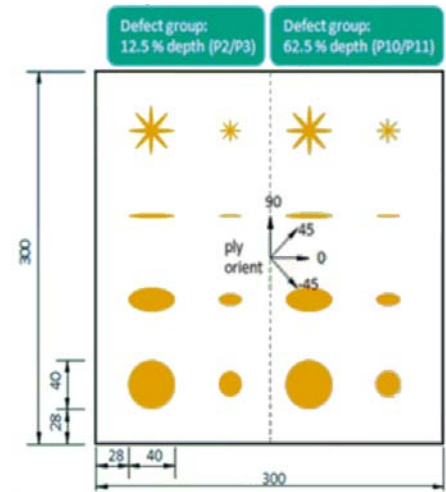Fig. 1   CFRP specimen of inclusion defects

Fig. 2   GFRP specimen of inclusion defects

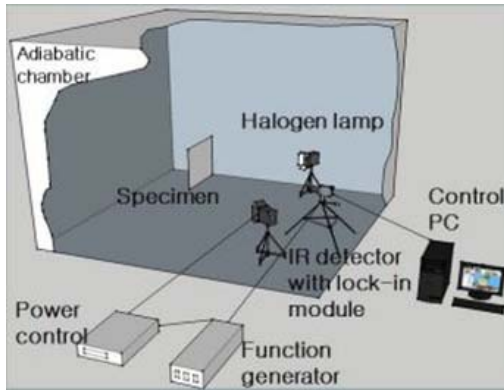
Fig. 3   Black matt painted specimen
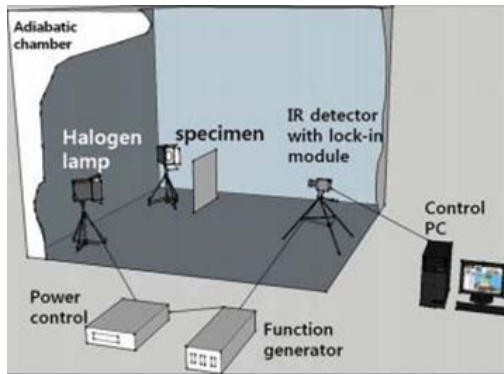
Fig. 4 Reflection method

Fig. 5 Transmission method

The images of 3600 frames were acquired in 60 frames per second by using FLIR's Silver 480 (NETD 25 mK). In addition, digital lock-in pulse thermography for signal processing of thermal images was applied to the conventional optical infrared thermography system in order to detect defects in flat-plate composites effectively.

Infrared thermography equipment is composed of a light source heating device and an infrared thermography camera, and in order to minimize the heat exchange between the specimen and external heat source, the experimental device is configured inside the thermostatic chamber as shown in Fig. 4.

For light sources, two 1 kW halogen lamps were installed at a distance of 2 m and placed in experimental settings divided into reflection method and transmission method as shown in

Fig. 4 and Fig. 5 to compare the defects detection rate depending on the irradiation method.

In addition, the lock-in method used to increase the defects detection rate of flat-plate composites of inclusion defects is to modulate the heat source that stimulates the defect detection object into a harmonic function for incidence, synchronize the detection element on the harmonic function, demodulate the phase change of the harmonic function, and thus to collect images. It is used to improve the detection sensitivity and minimize the defects detection error caused by non-uniformity of the surface emissivity [5].

3. Theory of Thermal Wave and Lock in Thermography

3.1. Thermal Wave

The thermal diffusivity α_{diff} (1) is ratio of the thermal conductivity λ to the volumetric heat capacity (i.e., the product of specific heat capacity and density)

$$\alpha_{diff} = \frac{\lambda}{\rho c_p} \tag{1}$$

The thermal diffusivity is a measure of the thermal energy diffusion rate through the material. The diffusion rate will increase with the ability to conduct heat and decrease with the amount of thermal energy needed to increase the temperature. Large values of diffusivity mean that objects respond fast to changes of the thermal conditions. Therefore, this quantity governs the time scale of heat transfer into materials. If a material has voids or pores in its structure, then the thermal conductivity and density decrease, which means the thermal diffusivity changes. As a result, the heat transfer within the material is affected, leading to observable changes of surface temperatures in the vicinity of the defects.

The thermal effusivity e_{eff} (2) is defined as the square root of the product of the thermal conductivity and the volumetric heat capacity.

$$e_{eff} = \sqrt{\lambda \rho c_p} \qquad (2)$$

It is a heat transfer property that determines the interfacial temperature when two semi-infinite objects at different temperatures touch. The effusivity also has another effect on heat transfer within a material.

As a mater of fact, one also often uses the concept of thermal waves in active thermography, in particular, of periodical heating processes are described, for example, in lock-in thermography [4,5].

It can be shown that the Fourier equation, assuming harmonic object heating at the surface provides a harmonic temperature field within the object with the same frequency but different amplitude and phase. Therefore, the concept of thermal waves, which and be described by the theory of wave physics, can be introduced. The main characteristic of thermal waves is the strong decay as a function of depth in the object. This decay can be characterized by the thermal diffusion length, which resembles a thermal penetration depth. μ (3) can give a first idea of possible depth ranges [6].

$$\mu = \sqrt{\frac{a_{diff}}{\pi f}} \qquad (3)$$

3.2. Lock in Thermography

Lock in thermography [7,8] is very similar tl pulse thermography in terms of the setup, however, the pulsed thermal excitation is replaced by a sinusoidal input of thermal energy. This is most easily realized by illuminating an extended sample by a modulated lamp. This periodic, to be specific harmonic, heating input leads to a similar transient harmonic variation of the surface temperature of the object. Harmonic
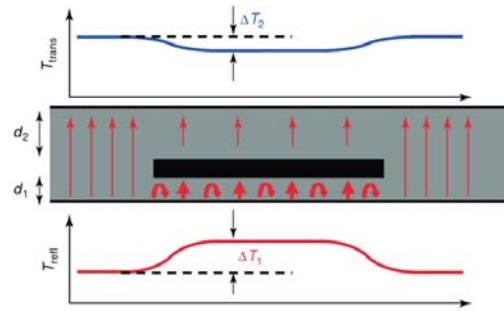

Fig. 6 Observable surface temperature differences depend of the thermal material properties of object and intrusion

heating at the surface also leads to harmonic temperature variations at given depths within the object, although with a strongly attenuated amplitude as a function of depth, described by the thermal diffusion length μ.

The amplitude and phase of a modulated thermal wave were extracted using correlation between two signals of thermal wave signal and a reference harmonic function at a narrow band since the algorithm applied in this work was DLICM method, By basically evaluating the harmonics of the thermal wave from carrying the dominant information, higher harmonics were suppressed. Also, using DLICM, it was realized by applying a synchronous correlation between thermal wave and a reference harmonic function. Where, as shown from Eqs. (5) and (6) So is the component of thermal signal by the sine function, and $S\pi/2$ is the component of thermal signal by the sine function like equation, The amplitude and phase of modulated thermal wave signal A(x, y, z) are decided from the sine and cosine correlations which take account the phase of the thermal wave signal, Here, two-channel correlation including

two reference sine and cosine functions are applied. One channel calculates the component of thermal wave signal by sine function, the other calculates the component by cosine function [9]

$$R_s(n) = \cos\left(2\pi\frac{n-1}{N}\right), \ \ n = 1,2,3,...N \quad (4)$$

$$S_0 = Corr[A(x,y,n), R_s(n)]$$
$$= \frac{c}{N}\sum_{n=1}^{N} A(x,y,n)\sin\left(2\pi\frac{n-1}{N}\right) \quad (5)$$

$$S_{\pi/2} = Corr[A(x,y,n), R_s(n)]$$
$$= \frac{c}{N}\sum_{n=1}^{N} A(x,y,n)\cos\left(2\pi\frac{n-1}{N}\right) \quad (6)$$

As corr at Eqs. of (4), (5) and (6) is reference operator indicating the correlations and c is the scale constant, the amplitude and the phase for A(x, y, n) can be obtained by following equations of (7).

$$A_s(x,y) = \sqrt{S_0^2 + S_{\pi/2}^2}, \phi(x,y) = \tan^{-1}\left\{\frac{S_{\pi/2}}{S_0}\right\} \quad (7)$$

4. Experimental Considerations

Fig. 7 shows defect images of specimens measured by the reflection method. In CFRP specimens, the irradiation time did not have a significant impact on the defects detection rate, and it was observed that the position and shape of the defects located in the right side at a depth of 50% were faintly detected. However, in the case of GFRP specimens, it was impossible to detect defects at the irradiation time of 300 mHz, and only the shape of the defect in the right side was faintly detected at 50 mHz. This is due to the results caused by the difference of thermal diffusivity among the properties of the composites. The thermal diffusivity of CFRP with a carbon content of 50 % is 3.3×10^{-7} m/s^2 [10], and GFRP has a value of 1.77×10^{-7} m/s^2 [11]. This indicates that the thermal diffusivity of CFRP is two times faster than that of GFRP. This characteristic serves to vary the time and the depth of penetration into the specimens where defects are present and thereby affects the detection of defects.
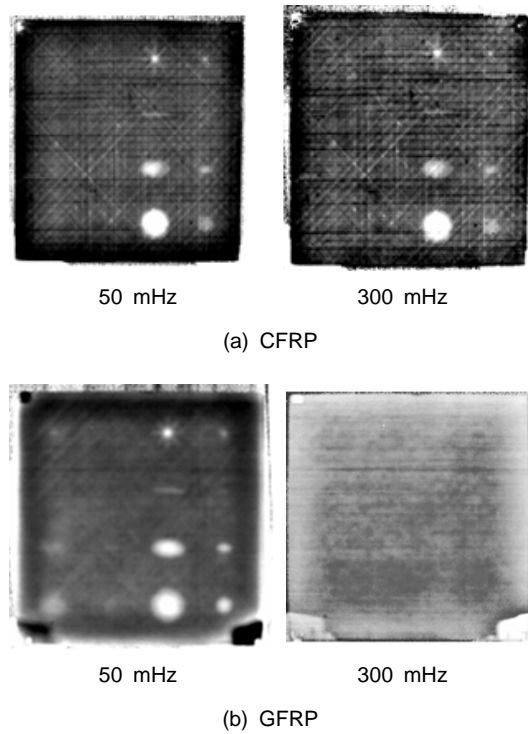

50 mHz   300 mHz

(a) CFRP

50 mHz   300 mHz

(b) GFRP

Fig. 7   Reflection method

50 mHz   300mHz

(a) CFRP

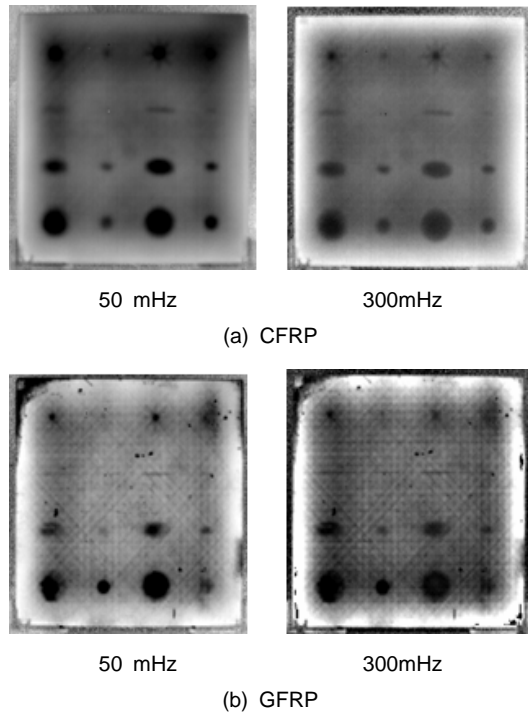

50 mHz   300mHz

(b) GFRP

Fig. 8   Transmission method

The thermal diffusion length depends on the thermal diffusivity a_{diff} and the frequency f of the thermal wave (of heat stimulation). This expresses the fact that low-frequency thermal waves will penetrate deeper into a material than the high-frequency waves. The penetration depth will increase with increasing diffeusivity, μ can give a first idea of possible depth ranges. Fig. 6 depicts a second example. A solid material 1 characterized by thermal diffusivity $a_{diff,1}$, conductivity λ_1, and effusivity $e_{eff,1}$, and so on has a subsurface structure of material 2, characterized by different values of thermal diffusivity $a_{diff,2}$, conductivity λ_2, and effusivity $e_{eff,2}$, Heat flow is induced by a thermal rectangular pulse from the bottom. If the effusivity $e_{eff,2}$ of the substructure is much lower than the one of material 1, the heat flow will try to at least partially bypass th obstacle, that is, it will be lower behind the substructure. At the same time, blocking of heat flow by the obstacle (visualized by the curved arrows) leads to lower heat flow from the surface to the inside of the material. As a consequence, the surface temperatures at the bottom of the thermal energy input will decrease more slowly in the region of the intrusion, that is, the temperature profile across the structure will lead to a temperature rise above the region of intrusion. In contrast, the corresponding heat flow is lower on the opposite side, giving rise the a lower temperature with regard to adjacent parts of the object. Depending of the distance of the obstacle from the two surfaces, the temperature profiles will differ: the don at greater distance will be shallower owing to lateral spreading by thermal diffusion within the material. In case the intrusion is of a material with much higher effusivity than the surrounding material 1, the respective temperature profiles from front and back would be inverted. If the distances d1 and d2 from the intrusion to object

surfaces are different, the temperature profile for the larger distance will, on the one hand, be more smeared out laterally due to the diffusion and, on the other hand, its thermal contrast will be lower [6].

The experiment confirmed that as the excitation time is longer, the penetration depth of heat is deepened, which makes it easier to detect defects. Especially in the case of reflection method, as the excitation time of heat is the same as the measurement time, thermal diffusion and radiation takes place in the same measurement surface.

This state is continuously subjected to the impact of thermal energy remaining at the time of measuring the radiation energy in an unheated state after the heat penetration into the measurement surface. However, as shown in Fig. 8 in the case of transmission method, as the excitation direction of heat and the measurement time appear differently, the measurement surface is different from the heating zone, which facilitates the detection of defects, and that is closely related to the diffusion direction of the thermal energy. Even in the experimental results, the transmission method exhibited higher defects detection rate regardless of the irradiation time and materials of the composites.

5. Quantitative Defects Detection

For quantification of defect size as shown in Fig. 9, a binarization process was performed using a self-developed defects quantification program in order to clarify the boundaries of the defective area and sound area. After the binarization process, the boundaries were distinguished clearly, and thus the length corresponding to 1 pixel was calculated to quantify the defect size using the length of 1 pixel and the number of pixels occupied by the defect.

Table 1 and 2 shows the results of defects quantification using defect images of CFRP
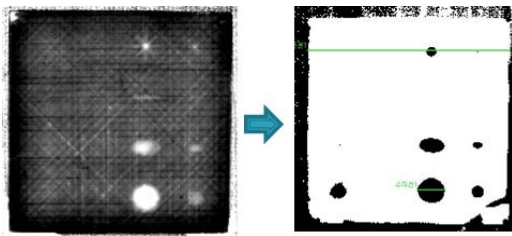
Fig. 9 Process of defects quantification

Table 1 Defects quantification results

Time	CFRP		
	Transmission method		
	Real size	Binarization	Gap
50 mHz	40 mm	39.88 mm	0.12 mm
300 mHz	40 mm	41.34 mm	1.34 mm

Table 2 Defects quantification results

Time	GFRP		
	Transmission method		
	Real size	Binarization	Gap
50 mHz	40 mm	39.77 mm	0.23 mm
300 mHz	40 mm	38.38 mm	1.62 mm

specimens in the transmission method that exhibited the highest defects detection rate. The quantification was performed by selecting the largest circular-shaped defect within the specimens.

When compared to the actual defect size, the quantified defect size was found to have a margin of error ranging from 1.34 mm to 0.12 mm and show high defects quantification accuracy of more than 95% at 50 mHz and 300 mHz.

6. Conclusion

This paper confirmed that in the case of CFRP and GFRP specimens of inclusion defects, the defects detection rate varies depending on the irradiation time, irradiation method and materials of composites. In addition, high accuracy of up to more than 95% was confirmed as a result of the study to quantify the defect size using the self-developed defects quantification program.

1) In the case of CFRP composite material laminated with eight layers with a thickness of 1.4 mm, the position and shape of the defect was more clearly observed in the transmission method than in the reflection method, and the irradiation time was found not to have a significant impact.

2) When measured by the reflection method, only the defect in the right side at a depth of 20% was faintly observed in both CFRP and GFRP composites, and it was impossible to detect defects at 300 mHz in the case of CFRP composite material.

3) In the case of GFRP composite material laminated with 16 layers with a thickness of 1.4 mm, the transmission method exhibited a high defects detection rate regardless of the irradiation time. In addition, a higher defects detection rate was achieved at 50 mHz in the reflection method.

4) CFRP specimen which showed the highest defects detection rate in quantification of the defect size also exhibited a high accuracy of up to more than 95% at 50 mHz in the transmission method.

Acknowledgement

References

[1] G. Gaussorgurs, "Infrared Thermography," Translated by S. Chomet, Champman & Hall, London, pp. 415-452 (1994)

[2] X. P. V. Maldague, "Theory and Practice of Infrared Technology for Nondestructive Testing," John Wiley & Sons, New York (2001)

[3] G. Busse, D. Wu and W. Karpen, "Thermal wave imaging with phase sensitive modulated thermography," *J. Appl. Phys.,* Vol. 71, No. 8, pp. 3962-3965 (1992)

[4] V. P, Vavilov, "Infrared and thermal testing: heat transfer," *Nondestructive Testing Handbook Series Ⅲ (3rd Ed.)*, X. P. V. Maldague, P. O. Moore Ed., ASNT, Columbus, USA, pp. 54-86 (2001)

[5] M. Y. Choi, H. S. Park, J. H. Park, W. T. Kim and W. J. Choi. "Study on the qualitative defects detection in composites by optical infrared thermography," *Journal of the Korean Society for Nondestructive Testing*, Vol. 31, No. 2, pp. 150-156 (2011)

[6] M. Vollmer and K.-P. Mollmann, "Infrared Thermal Imaging: Fundamentals, Research and Applications," John Wiley & Sons, pp. 220-224 (2010)

[7] P. O. Moore (ed.), Nondestrucive Testing Handbook, 3ʳᵈ American Society for Nondestructive Testing, Columbus (2001)

[8] O. Breitenstein and M. Langernkamp, "Lock-in Thermography," Springer-Verlag, Berlin and Heidelberg (2003)

[9] J. Liu, Y. Wang and J. Dai, "Research on thermal wave processing of lock-in thermography based on analyzing image sequences for NDT," *Infrared Phys. Technol*. Vol. 53, Issue 5, pp. 348-357 (2010)

[10] M. Navarrete, F. Serrania, M. Villagran, "Application of the flash method for the thermal characterization of woven carbon fibre laminates," *Materials and Design,* Vol. 22, pp. 93-97 (2001)

[11] G. Wróbel, S. Pawlak and G. Muzia. "Thermal diffusivity measurements of selected fiber reinforced polymer composites using heat pulse method," *Archives of Materials Science and Engineering*, Vol. 48. Issue 1, pp. 25-32 (2011)